International Journal of Pharmaceutics 532 (2017) 345–351

Contents lists available at ScienceDirect

International Journal of Pharmaceutics

journal homepage: www.elsevier.com/locate/ijpharm

The *in vivo* transformation and pharmacokinetic properties of a liquid crystalline drug delivery system

Andrew Otte[a,*], Yahira M. Báez-Santos[a], Ellina A. Mun[a], Bong-Kwan Soh[b], Young-nam Lee[b], Kinam Park[a,c]

[a] Purdue University, Weldon School of Biomedical Engineering, West Lafayette, IN 47907, USA
[b] Chong Kun Dang Research Institute, 315-20, Dongbaekjukjeondaero, Giheung-gu, Youngin-si, Gyeonggi-do, 16995, South Korea
[c] Purdue University, Department of Industrial and Physical Pharmacy, West Lafayette, IN 47907, USA

ARTICLE INFO

Keywords:
Liquid crystal
SAXS
Subcutaneous drug delivery
Sustained-release
Hexagonal mesophase
Leuprolide

ABSTRACT

A liquid crystalline (LC) system, composed of phosphatidylcholine, sorbitan monoleate, and tocopherol acetate, was investigated to understand the *in vivo* transformation after subcutaneous injection, coupled with the physicochemical and pharmacokinetic properties of the formulation. The rat model was utilized to monitor a pseudo-time course transformation from a precursor LC formulation to the LC matrix, coupled with the blood concentration profiles of the formulations containing leuprolide acetate. Three formulations that result in the H_{II} phase, demonstrating dissimilar *in vitro* release profiles, were used. The formulation showing the highest AUC, C_{max} and T_{max}, also displayed the greatest release rate *in vitro*, the lowest viscosity (LC matrix), and an earlier transformation (LC precursor to matrix) *in vivo*. A potential link between viscosity, phase transformation, and drug release properties of a liquid crystalline system is described.

1. Introduction

In situ forming implants (ISFI) are typically described as a polymer-based solution system that subsequently undergoes a process of solidification or phase inversion, after injection in the subcutaneous (SQ) space (Dunn et al., 1990). Upon SQ injection, the polymer forms a gel or precipitates as the temperature changes or water miscible solvent leaches out into the SQ space and water diffuses into the polymer system. Liquid crystalline (LC) systems are similar to polymer-based ISFIs. Upon injection into the subcutaneous space of a LC precursor solution, solvent diffuses out and water diffuses inward simultaneously, coupled with an additional 'crystallization/molecular rearrangement' into a LC matrix. The resulting system delivers the loaded drug molecule via diffusion through the submicron-sized water channels and biodegradation/erosion of the system (Boyd et al., 2006; Ki et al., 2014). Common mesophases that have been studied in drug delivery applications are the bicontinuous cubic and inverted hexagonal (H_{II}) structures. The unique microstructure of the LC matrix allows modification of the release rate through alteration of the composition and/or phase. It is well known that the drug release kinetics from poly(lactide-co-glycolide) (PLGA)-based systems depends on the polymer type (Astaneh et al., 2009; DesNoyer and McHugh, 2001), solvent (Brodbeck et al., 1999), additives (Bakhshi et al., 2006; Graham et al., 1999), and drug properties (Solorio et al., 2012b). Similar effects have also been found in LC systems (Boyd et al., 2006; Chang and Bodmeier, 1998; Dong et al., 2006). In addition, changes in the polymer implant microstructure that occurs *in situ* can significantly alter the drug release and degradation rate of the implants (Solorio and Exner, 2015). Furthermore, the increased interstitial pressure, compressive forces from tissue, and potential mechanical/physical impact on the injection site due to everyday activities are likely to lead to increased efflux of solvent and drug, and enhanced possibility of breakage/erosion of the liquid crystal depot itself, relative to its *in vitro* counterpart (Patel et al., 2010). To date, very few published studies exist documenting the *in vivo* behavior and/or pharmacokinetic properties after SQ or intramuscular (IM) injection of LC systems, particularly in regards to the wide array of LC systems that have been documented and published. Tiberg et al. showed that the FluidCrystal® system post injection gave stable and dose-dependent leuprolide plasma values for a month, after which the release decays rapidly as the depot degrades and becomes completely empty (Tiberg and Joabsson, 2010). Other leuprolide delivery systems based on PLA/PLGA microspheres and gels have a more pronounced initial burst release, followed by lower and less stable plasma concentrations over time. Understandably, the composition of the FluidCrystal® formulation is usually not presented, making it difficult to interpret the relationship between the drug loading, structure,

* Corresponding author.
E-mail address: aotte@purdue.edu (A. Otte).

http://dx.doi.org/10.1016/j.ijpharm.2017.08.098
Received 6 June 2017; Received in revised form 2 August 2017; Accepted 20 August 2017
Available online 24 August 2017

transformation, and subsequent release curves.Fong et al. used glucose as a model hydrophilic drug and demonstrated that drug diffusion was reversible on switching between the H_{II} and Q_2 nanostructures at temperatures above and below physiological temperature, respectively (Fong et al., 2009). An *in vivo* proof of concept study in rats showed that after SQ administration of these materials, the changes in nanostructure induced by application of a heat or cool pack at the injection site stimulated changes in drug release from the matrix anticipated from *in vitro* release behavior, thereby demonstrating the potential utility of these systems as 'on demand' drug release delivery vehicles. Although the formation of Q_2 or H_{II} has not been directly verified *in vivo* in this study, the systematic increases in t_{max} in the current study after administration of model drug from aqueous solution to Q_2 to H_{II} precursor systems supports the concept that the slow *in vitro* release from the Q_2 phase, and slower from the H_{II} phase, leads to differences in absorption rate and appearance in plasma. Previous works by Ki et al. and Lim et al. performed pharmacokinetic studies in rats and dogs using a hexagonal liquid crystal system of sorbitan monooleate, phosphatidycholine, tocopherol acetate, and Tween 80, delivering leuprolide for 28 days and entecavir for 3-5 days, respectively (Ki et al., 2014; Lim et al., 2015). In this work, 3 ternary formulations of phosphatidylcholine (PC), sorbitan monooleate (SMO), and tocopherol acetate (TA) were used to determine their potential *in vivo* transformation and pharmacokinetic profiles of leuprolide acetate. Three ratios of PC:SMO:TA, 50:30:20, 60:30:10, & 60:40:0, were chosen for this experiment based on the *in vitro* release profiles from a previous study (Báez-Santos et al., 2016). The goal of this study is to examine an *in vitro-in vivo* correlation (IVIVC) using parameters, such as the LC structure, leuprolide release kinetics, and their physicochemical characteristics. The hypothesized transformation mechanism post injection is that water diffuses into the LC depot and solvent diffuses out simultaneously, coupled with molecular rearrangement into a 3D LC matrix. From this rearranged structure, drug diffuses out of the tortuous network of nano-sized water channels. There have been no published articles demonstrating the actual *in vivo* transformation of a SQ injected LC system along with the drug release that may occur due to the fluid movement and structural rearrangement. A feature that distinguishes injectable drug delivery systems is that a critical aspect of its initial drug release occurs simultaneously with the formation of the device by phase inversion (Graham et al., 1999). Thus, controlling the drug release characteristics requires understanding of the dynamics of the *in vivo* phase separation process (Graham et al., 1999).This work demonstrates how the ternary components influence the physicochemical and structural properties and their subsequent effect on the *in vitro* release, as well as *in vivo* pharmacokinetic properties, providing a means of evaluating formulation variables in a pre-clinical setting. A link between the viscosity of a LC matrix, the structural transformation "rate," and *in vitro* release to the *in vivo* pharmacokinetic profile was found. It is hypothesized, based on these results, that controlling the drug release in the hexagonal phase requires a critical viscosity/intermolecular bonding strength. It is likely that the leuprolide release occurs by combination of diffusion through membrane bilayers, diffusion through the aqueous channels, and erosion/degradation of the LC matrix.

2. Materials and methods

2.1. Materials

Leuprolide acetate, sorbitan monooleate (SMO) (Montane™ 80), tocopherol acetate (TA) and soy phosphatidylcholine (PC) (Lipoid S100) were purchased from Polypeptide Group (San Diego, CA, USA), Seppic (Puteaux, France), DSM Nutritional Products Limited (Sisseln, Switzerland), and Lipoid GmBH (Ludwigshafen, Germany), respectively. All other chemical and reagents were of analytical grade and were purchased from Sigma-Aldrich or Fisher Scientific.

2.2. Preparation of liquid crystalline systems

The bulk phase vehicle consists of mixing SMO, PC, and TA in their respective ratios based on the formulation, along with ethanol at 10% (w/w) according to the method described previously (Ki et al., 2014). In brief, SMO, PC, TA, and ethanol were weighed in a 20 mL scintillation vial and mixed at room temperature overnight on a vortex shaker. The leuprolide acetate solution was prepared by dissolving 3.75 mg of leuprolide acetate in 5 μL of DMSO. The final LC formulation was designed to contain 3.75 mg of leuprolide acetate totaling a volume of 100 μL.

2.3. Rheological characterization

Rheological measurements were carried out with a TA Instruments ARES Rheometer. Samples were placed in excess water for 7 days and the excess water was removed 24 h prior to measurement via centrifugation and stored at 25 °C. 40 mm parallel plates were used for the characterization. The sample thickness was 1.5 mm. The samples were gently inserted onto the top of the bottom plate, and the top plate was slowly moved to the 1.5 mm measurement distance. Any sample that squeezed out from between the plates was gently removed. Measurements began after an equilibration time of 10 min to allow for stress relaxation. Measurements were carried out at 25 °C. Steady shear measurements were performed on all the samples using shear rates from 0.01 to 100 s^{-1}.

2.4. Subcutaneous rodent injections for SAXS determination

100 μL of formulation was injected subcutaneously in the rat. Injections were performed 7, 3, and 1 day prior to SAXS measurements as a means to observe the pseudo-time course subcutaneous transformation of the LC vehicle to matrix formulation. Three different rats were injected with Formulations F4, F7, & F8 on each day (F4, F7, & F8 are the same formulation designations from the previous study (Báez-Santos et al., 2016)). The LC matrix was removed from the rat prior to the SAXS measurement, and in most cases, some surrounding SQ tissue was attached to the LC matrix. While every attempt was made to remove all subcutaneous tissue without disrupting the LC, some tissue still may have remained with the LC matrix. The LC depot was then lightly sandwiched between a glass slide and cover slip and sealed with vacuum grease to prevent any environmental changes that may affect the LC. The Purdue Animal Care and Use Committee (PACUC) reviewed and approved the study protocol.

2.5. Small angle X-ray scattering (SAXS) measurements

The synchrotron beamline 12-BM-B at the Advanced Photon Source (APS), Argonne National Laboratory, was used for SAXS measurements. Samples were prepared as described above, according to the ternary phase diagram composition ratios. LC precursor was added to excess simulated body fluid (SBF) buffer and vigorously mixed on a vortex shaker for 1–3 min to ensure homogenization. In vitro samples were allowed to equilibrate for at least seven days prior to SAXS analysis. *In vitro* samples were loaded into the backend of a syringe with a spatula and carefully injected and packed into the capillary tubes with a 1.5" 16 G needle and sealed with wax. *In vitro* samples were then placed in 1.5 or 2.0 mm diameter Boron Rich capillary tubes (Charles Supper Co. Natick, MA, USA) and inserted into a block sample holder. The *in vivo* samples sandwiched between glass slides were positioned vertically and normal to the incident X-ray beam. SAXS data were collected at room temperature by exposing the sample to the 12.0 keV (1.0332 Å) X-ray beam. Depending on the sample's scattering intensity, exposure times of 1 to 5 s per frame were found optimal to maximize signal-to-noise ratio while minimizing X-ray radiation damage. X-ray scatter from the sample were recorded using a MarCCD 165 detector positioned at a

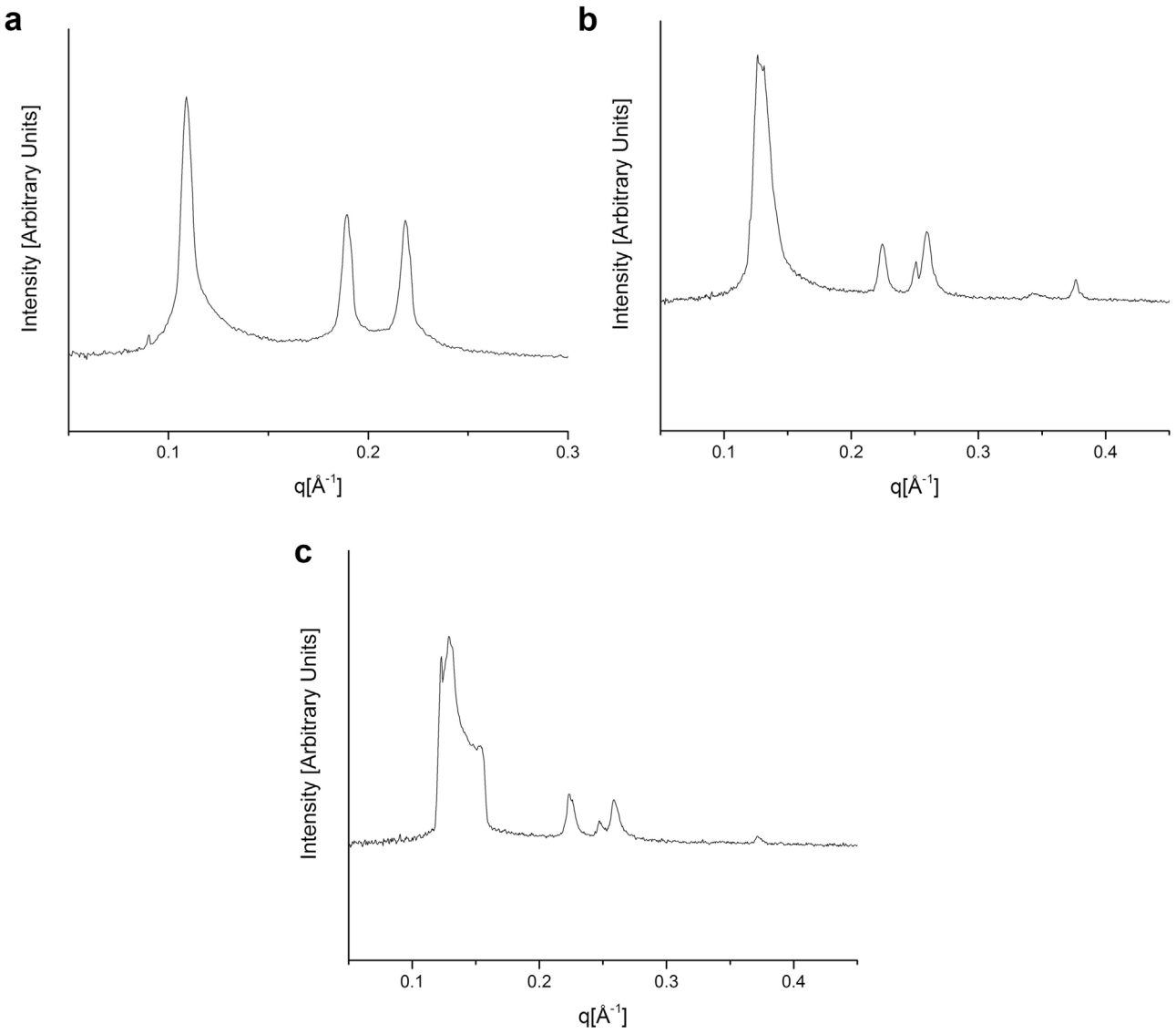

Fig. 1. *In vitro* SAXS profiles. The formulation ratios listed are for PC/SMO/TA. (A) F4 – 50/40/10 (B) F7 – 60/30/10 (C) F8 – 60/40/0.

sample-to-detector distance of 1.182 m. Silver behenate was used for the angular detector calibration (Huang et al., 1993).

Data reduction of the two-dimensional (2D) SAXS patterns were processed using the Nika Package (Ilavsky, 2012) from Irena to obtain one-dimensional (1D) data in the form of scattered intensity versus scattering vector, q, given by Eq. (1)

$$q = \left(\frac{4\pi}{\lambda}\right)\sin(\theta/2) \tag{1}$$

where λ is the wavelength of the incident X-rays and 2θ is the scattering angle relative to the incident of the X-ray beam. A q-range of $0.01 \sim 4.0\ \mathrm{nm}^{-1}$ was used for all data collected. Bragg's law was used to analyze resulting scattering profiles based on the d-spacing and is given by Eq. (2)

$$n\lambda = 2d\sin(\theta) \tag{2}$$

where n is the scattered peak order and the lattice parameter, d, is the interplanar spacing or the distance between the centers of adjacent cylinders of the H_{II} mesophase, obtained by combining Eqs. (1) and (2) as shown in Eq. (3)

$$d = 2\pi/q \tag{3}$$

Identification of the LC mesophases was based on the relative position of the Bragg peaks on the scattering vector axis. SAXS patterns with q-spacing ratios of 1:√3:√4:√7, etc. correspond to H_{II} mesophase, whereas ratios of 1:2:3:4, etc. correspond to L_α mesophase (Holmberg et al., 2002).

2.6. *In vivo* pharmacokinetic analysis

The LC precursor material containing 3.75 mg of leuprolide acetate was injected into the SQ space of the rat's lower back. The Culex NxT™ with Raturn® was used for the pharmacokinetic study as means to automatically collect the blood samples. Samples were collected from the catheter at 0, 0.5, 1, 3 and 24 h and 2, 3, 4, and 7 days post injection. Each blood sample was mixed with Na-heparin, resulting in 15 IU/mL of Na-heparin in blood and centrifuged at 4 °C and 4000 rpm for 20 min. The centrifuged plasma samples was mixed with 100 µL of aprotinin solution (30 TIU/5 mL) and stored at −80 °C prior to analysis.

An internal standard solution containing 20 µL of Cetrorelix (50 ng/mL in 50% methanol:50% water) was added to 50 µL plasma and vortexed. Protein precipitation was performed by adding 200 µL of acetonitrile. The mixture was vortexed and then centrifuged at 15,000*g* for 10 min. The supernatant was collected and dried under low pressure centrifugation. Samples were reconstituted in 100 µL of 50% ACN:50%

water, sonicated, and centrifuged at 13,000*g* for 5 min. Supernatant was transferred to HPLC vials prior to for HPLC/MS–MS analysis.

Leuprolide concentrations in plasma were quantitated by HPLC/MS-MS. Separation was performed on an Agilent Rapid Res 1200 HPLC system using an Agilent Zorbax XDB C18 (2.1 × 50 mm, 3.5 µm) column. Mobile phase A was water with 0.1% formic acid and mobile phase B was acetonitrile with 0.1% formic acid. A linear gradient elution was used as follows: initial condition 5% B; 1–5 min, 100% B; 5–9 min, 100% B. Column re-equilibration was 9–10 min, 5% B; 10–15 min, 5% B. Column flow rate was 0.3 mL/min. Retention time for leuprolide and cetrorelix was 6.7 min and 7.2 min, respectively. MS/MS utilized an Agilent 6460 Triple Quadrupole mass spectrometer, with positive electrospray ionization (ESI). Quantitation was based on Multiple Reaction Monitoring (MRM). For leuprolide, transitions were 605.5 to 249.1 and 605.5 to 221.1, at collision energy of 30 and 40, respectively. For cetrorelix, transitions were 716.1 to 694.6 and 716.1 to 154.1, at collision energy of 20 and 40, respectively. Quantitation was based on a 4-point standard curve, with leuprolide concentrations ranging from 0.2 to 200 ng/mL. The standard curve was prepared in unmedicated rat plasma. Responses for leuprolide were normalized against the cetrorelix internal standard. A quadratic fit was applied, with a 1/x weighting, resulting in a $R^2 = 0.999$

3. Results and discussion

3.1. In vitro SAXS

Formulations F4, F7, and F8 showed a transformation into a LC matrix when exposed to excess SBF buffer. Only Formulation F4 transformed into the hexagonal phase, whereas F7 and F8 showed a mixture of H_{II} and lamellar L_α phases or H_{II} only (Fig. 1), depending on the location of the LC matrix where the SAXS pattern was obtained. The L_α phase has been described as a precursor phase to the H_{II} phase, where line defects lead to the formation of the first rods (Siegel, 1986), aggregation of transmonolayer contacts (Siegel and Epand, 1997), or a cooperative chain reaction of rod formation at the transition midpoint (Rappolt et al., 2003). In this instance, it is hypothesized that the mixture of H_{II} and L_α phases is most likely due to an inhomogeneity throughout the LC matrix, due to a lack of sufficient molecular interactions between the components based on their ternary ratios.

3.2. In vitro release profiles

The *in vitro* release profiles for formulations F4, F7, & F8 are shown in Fig. 2. These release profiles demonstrated vastly different release profiles for the 3 formulations as precursor oil only, and when the mesophase at 13% aqueous content was tested, this further showed differences in the release profiles (Báez-Santos et al., 2016). While the release method may have an impact on the results, as multiple release methods have been used in the literature, the trends of the overall release profiles of the formulations are not believed to deviate. In this method, samples were loaded into dialysis tubes and shaken in an incubator shaker at 100 RPM at 37 °C for 28 days. In this method, the LC stayed intact, whereas in other methods, it may break down into smaller pieces depending on the formulation used, due to varying levels of intermolecular interactions between the formulations based on their respective composition.

3.3. Rheological characterization

The major rheological properties of different LC phases depend mostly on the topology of the water-lipid interface (Mezzenga et al., 2005). Fan et al., found a typical shear thinning behavior for a hexagonal LC phase composed of Brij 97 and sodium deoxycholate mixtures (Fan et al., 2016). As expected, they also showed a decrease in viscosity as a function of temperature for the same composition. In addition, the increase in the water content within the same LC phase of a monoolein system caused an increase of the lattice constant at temperatures greater than 25 °C (Qiu and Caffrey, 2000), also potentially influencing the viscosity.In this study, the rheological behavior of three different formulations at their equilibrium water content values was studied. Fig. 3 shows the shear viscosity vs shear rate at 25 °C for the three formulations in question. The three formulations show typical shear-thinning behavior, but at higher shear rates, the viscosity of F8 drops dramatically, indicative of a potential lack of intermolecular interactions due to the absence of tocopherol acetate in this formulation or the higher water content relative to F4 and F7. F4 exhibits the highest viscosity over the entire shear rate range studied, where F7 was generally higher than F8 except some slight overlap at low shear rates.

3.4. In vivo structural transformation

No reports have been published to this date on the actual phase transformation of a LC system *in vivo*. In this study, a pseudo-time

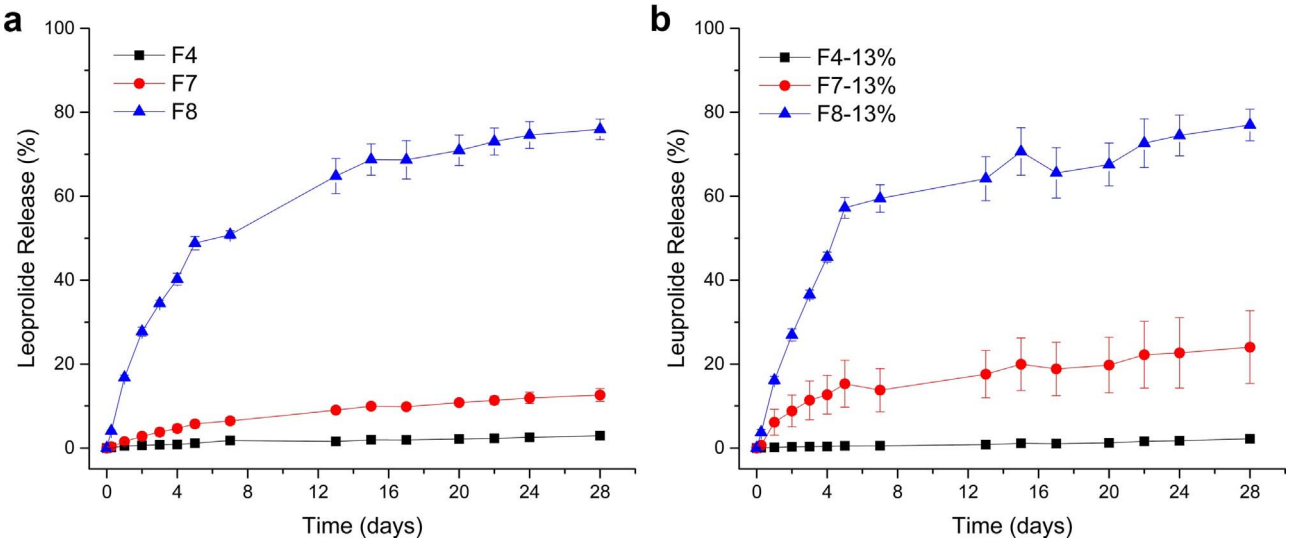

Fig. 2. *In vitro* release profiles of Formulations F4, F7, and F8 from the LC precursor (A) versus their respective mesophases at 13% (w/w) SBF (B). (Replotted with permission from (Báez-Santos et al., 2016)).

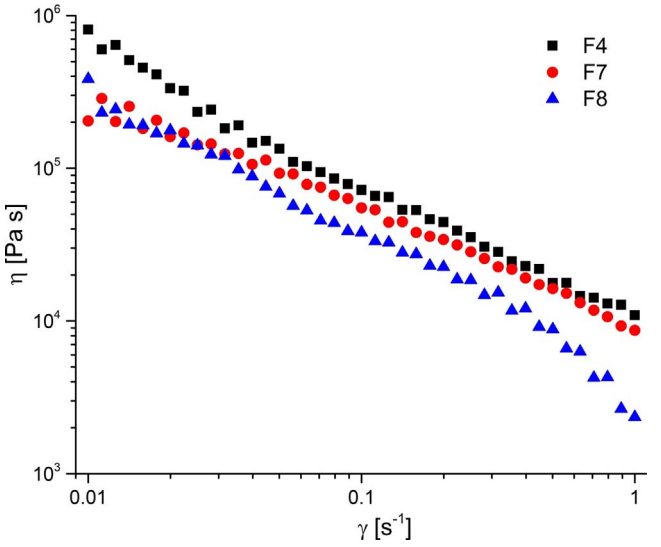

Fig. 3. The shear viscosity as a function of the shear rate for the three PC:SMO:TA formulations.

course study was performed to further understand the potential transformation *in vivo*. Ideally, these experiments would be performed without sacrificing the animal; unfortunately, however, SAXS is the main technique that will provide definitive structural information on the LC. Ultrasound experiments have been used to determine the extent of transformation of ISFIs (Solorio et al., 2012a, 2010). Preliminary ultrasound experiments have been performed to assess the *in vivo* transformation. During injection, the LC initially appears anechoic, due to the solvent nature, and there is a notable transition towards hypo-/hyperechogenecity even during injection. This could be due to solvent migration from the LC alone, and not simultaneous exchange between solvent and aqueous fluid along with the structural rearrangement. An alternative for future experimentation could be to couple the ultrasound experiments with spectroscopic imaging. Xu et al. used an *in situ* Kaiser Raman spectrometer probe to show LC formation of a 44% GDO, 44% SPC, and 12% ethanol solution from hydrogen out-of-plane wagging from $-CH_2$ in the lipid, where complete formation was noted in 8 h in a dialysis tube (Xu et al., 2016). In this study, rodents were sacrificed to examine the *in vivo* phase transformation of 3 formulations. Three rodents were injected with each formulation of interest 7 days, 3 days, and 1 day prior to the SAXS experiment. The LC was then carefully excised from the rodent. Some surrounding tissues visually appeared to merge with the LC material and any material that was readily excisable was removed with caution not to disturb the LC. The LC was then lightly placed between a glass slide and cover slip and immediately sealed with vacuum grease in an effort to prevent any moisture migration to/from the LC material. Due to the experimental nature, the thickness of the LC material during the SAXS experiments was not controlled in an effort to minimize disturbing the samples. At least 15 SAXS patterns were obtained throughout a LC depot as this number of patterns seemed adequate to sample the entire depot, with the results illustrated in Fig. 4. At Day 1, no diffraction patterns were detected in the depot for Formulations F4 and F7, whereas what appears to be a mixture of H_{II} and L_α was noted for F8. Identification of the LC mesophases was based on the relative position of the Bragg peaks on the scattering vector axis. SAXS patterns with q-spacing ratios of 1:√3:√4:√7, etc. correspond to H_{II} mesophase, whereas ratios of 1:2:3:4, etc. correspond to L_α mesophase (Holmberg et al., 2002). For F4, a H_{II} phase was then found at Day 3 and Day 7. For F7, a H_{II} and a mixture of H_{II} and L_α was noted at Day 3 and only a H_{II} phase was noted at Day 7. For F8, no phase was detected at Day 3 and Day 7. The water uptake data show that F4, F7, and F8 gained 10.6%, 16.8%, and 30.8% water at 1 h and their equilibrium water content values were 23.1%, 36.8%, and 44.4%, showing faster *in vitro* water uptake for F8 as compared with that for F4 and F7. Formulation F8 absorbed 69% of the equilibrium water uptake in 1 h, while the other two formulations absorbed only 46% of the equilibrium values. Since it was not possible to remove all surrounding tissue from the LC depot without potentially disturbing the depot, measurements may have been interfered with by the tissue. In addition, the lack of any diffraction patterns does not imply the complete lack of transformation from LC precursor to matrix. While it is possible, although unlikely, that only an extremely small portion of the LC depot transformed. Determining the percentage of "crystallinity" in these samples was not possible with the method used. Thus, it is not known whether these samples are in thermodynamic equilibrium; the method simply provides information as to whether a LC phase was/was not detected in the sample. These measurements, based on the experimental protocol used, appear to show that this LC precursor does in fact transform to a LC matrix in the subcutaneous space (Fig. 5).

3.5. *In vivo* pharmacokinetic profiles

Finally, pharmacokinetic studies were performed to assess the release profiles from the LC systems, in an attempt to bridge the gap between the *in vitro* and *in vivo* characterization. Rats were injected in the lower SQ space of the back and blood samples were taken over a week. The resultant leuprolide plasma concentration profiles of the three formulations are shown in Fig. 4. Calculated pharmacokinetic parameters from the data in Fig. 4 are also shown in Table 1.Formulation F8 exhibits the largest burst release followed by F7 and then F4. After the first 24 h "burst" release phase, minimal drug release occurs over the next 6 days (~43%, 16%, and 2% for F4, F7, and F8, respectively) relative to the first 24 h. Only limited *in vivo* data exist in the literature for comparison. Ki et al., provides a similar formulation to F4, but it also contains 2% Tween 80 in addition to the ternary components, potentially accounting for the vastly different sustained release profile, considering the effects Tween 80 has on the *in vitro* release profile (Ki et al., 2014). Secondly, if release of a hexagonal system is through membrane bilayers, with leuprolide being a large molecule and loaded at 3.75%, it is plausible to assume that very minimal drug release may occur and nearly all drug may be trapped inside the "shell" of the LC.Based on the respective ratio of components in this three component LC ternary mixture, very different initial release profiles were obtained, potentially due to the transformation and or viscosity/strength of the LC matrix. While all 3 formulations had relatively similar t_{max} values (Table 1), both C_{max} and *AUC* were vastly different between the 3 formulations. Interestingly, in contrast to F7 and F8, very little drug is released from Formulation F4. This may show the significance of the role of degradation/erosion of these systems, coupled with the sustained release capabilities. If F8 was assumed to reach 100% release in 7 days, F4 still has ~93% drug remaining in the system. This data highlights the importance that minor changes in a LC formulation can have an extremely large influence on the release kinetics. While the viscosity of the LC formulation is important, potentially of equal importance may be the phase transformation kinetics, the mechanism of transformation, and/or the erosion/degradation kinetics. In addition, the rat model used may not be the best model to describe this system. The LC system was essentially injected into the SQ 'space' of the animal, between the muscle and the skin. Although in humans, the injection site (typically back of arm or abdominal region) largely consists of adipose tissue. To better mimic the human conditions in an animal model, the porcine model or Zucker Diabetic Fatty rat may be a better research model for this type of drug delivery system.

4. Conclusions

Several conclusions can be drawn from this study. This study demonstrates that the ternary LC precursor in fact transforms into the respective LC matrix in the subcutaneous space. It is important to point

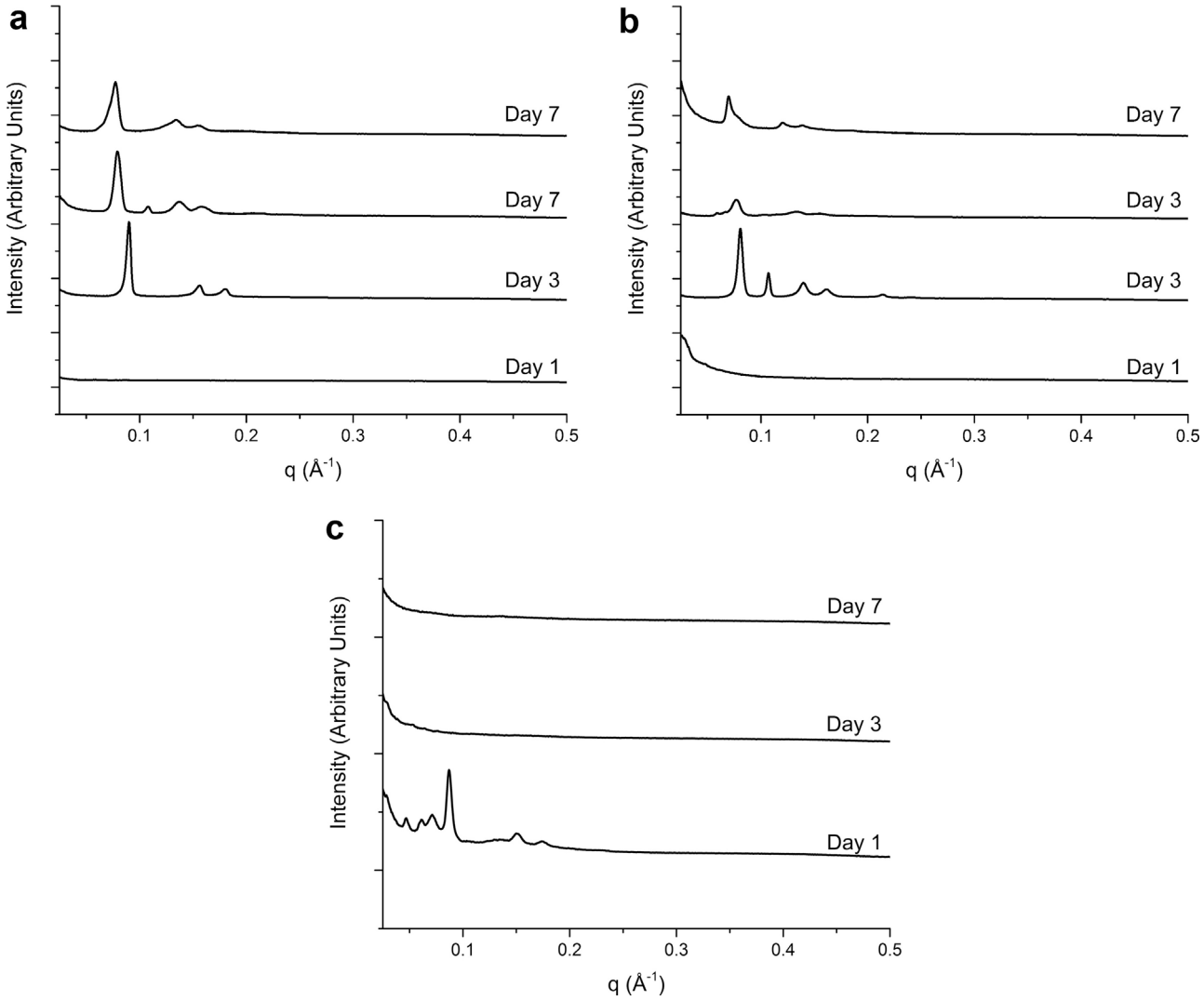

Fig. 4. Subcutaneous extracted LC *In vivo* SAXS patterns of the three PC:SMO:TA formulations as a function of time – (A) F4; (B) F7; (C) F8.

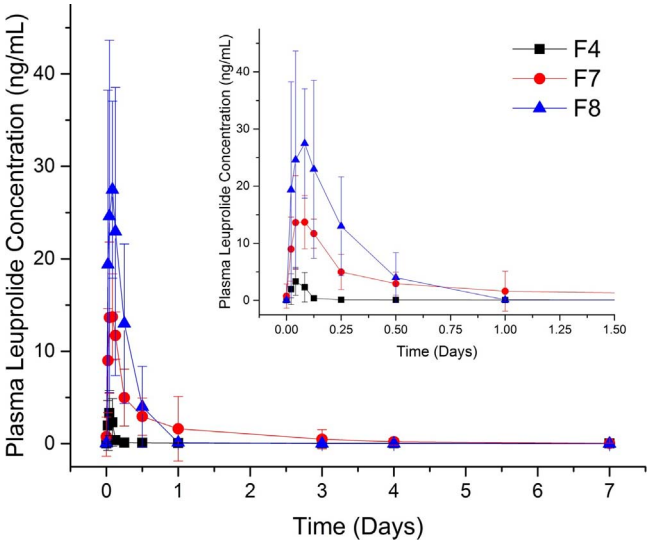

Fig. 5. Plasma concentration profiles of leuprolide acetate in rats for the three PC:SMO:TA formulations (n = 8).

out that the relative extent of *in vivo* transformation, e.g., precursor to actual matrix percentage, is still unknown. It is also important to consider the impact of degradation/erosion of these systems, since release of large molecules may only occur through breakdown and diffusion of the drug from the depot. This may be advantageous as an injection volume of only 100 µL may be able to delivery low dose compounds for months.

Table 1
Calculated pharmacokinetic parameters from the concentration-time profiles.

Formulation	F4	F7	F8
t_{max} (h)	1.31 ± 0.59	1.81 ± 0.92	2.42 ± 0.79
C_{max} (ng/mL)	3.65 ± 2.88	16.50 ± 6.16	34.77 ± 18.68
$AUC_{0\text{-}24}$ (h·ng/ml)	8.46 ± 6.03	103.07 ± 39.21	217.77 ± 82.84
$AUC_{0\text{-}168}$ (h·ng/ml)	14.85 ± 7.77	122.45 ± 43.58	222.80 ± 85.71

Acknowledgments

This research was supported by Chong Kun Dang Pharmaceutical Corp. We thank the beamline scientists at 12-BM-B at the Advanced Photon Source, an Office of Science User Facility operated for the U.S. Department of Energy (DOE) Office of Science by Argonne National Laboratory, which is supported by the U.S. DOE under Contract No. DE-AC02-06CH11357. We thank Robyn McCain of the Translation Pharmacology Core Facility and Bruce Cooper of the Metabolite

Profiling Facility in the Bindley Bioscience Center for the *in vivo* rat work and the mass spectrometry analysis respectively.

References

Astaneh, R., Erfan, M., Moghimi, H., Mobedi, H., 2009. Pharmaceutics, preformulation and drug delivery changes in morphology of in situ forming PLGA implant prepared by different polymer molecular weight and its effect on release behavior. J. Pharm. Sci. 98, 135–145. http://dx.doi.org/10.1002/jps.21415.

Báez-Santos, Y.M., Otte, A., Mun, E., Soh, B.K., Song, C.-G., Lee, Y., Park, K., 2016. Formulation and characterization of a liquid crystalline hexagonal mesophase region of phosphatidylcholine, sorbitan monooleate, and tocopherol acetate for sustained delivery of leuprolide acetate. Int. J. Pharm. 514, 314–321. http://dx.doi.org/10.1016/j.ijpharm.2016.06.138.

Bakhshi, R., Vasheghani-Farahani, E., Mobedi, H., Jamshidi, A., Khakpour, M., 2006. The effect of additives on naltrexone hydrochloride release and solvent removal rate from an injectablein situ forming PLGA implant. Polym. Adv. Technol. 17, 354–359. http://dx.doi.org/10.1002/pat.717.

Boyd, B.J., Whittaker, D.V., Khoo, S.-M., Davey, G., 2006. Lyotropic liquid crystalline phases formed from glycerate surfactants as sustained release drug delivery systems. Int. J. Pharm. 309, 218–226. http://dx.doi.org/10.1016/j.ijpharm.2005.11.033.

Brodbeck, K.J., DesNoyer, J.R., McHugh, A.J., 1999. Phase inversion dynamics of PLGA solutions related to drug delivery: part II. The role of solution thermodynamics and bath-side mass transfer. J. Control. Release 62, 333–344.

Chang, C., Bodmeier, R., 1998. Low viscosity monoglyceride-based drug delivery systems transforming into a highly viscous cubic phase. Int. J. Pharm. 173, 51–60.

DesNoyer, J.R., McHugh, A.J., 2001. Role of crystallization in the phase inversion dynamics and protein release kinetics of injectable drug delivery systems. J. Control. Release 70, 285–294. http://dx.doi.org/10.1016/S0168-3659(00)00354-0.

Dong, Y.D., Larson, I., Hanley, T., Boyd, B.J., 2006. Bulk and dispersed aqueous phase behavior of phytantriol: effect of vitamin E acetate and F127 polymer on liquid crystal nanostructure. Langmuir 22, 9512–9518. http://dx.doi.org/10.1021/la061706v.

Richard L. Dunn, James P. English, Donald R. Cowsar, D.P.V., 1990. Biodegradable in-situ forming implants and methods of producing the same.

Fan, J., Liu, F., Wang, Z., 2016. Shear rheology and in-vitro release kinetic study of apigenin from lyotropic liquid crystal. Int. J. Pharm. 497, 248–254. http://dx.doi.org/10.1016/j.ijpharm.2015.12.008.

Fong, W.-K., Hanley, T., Boyd, B.J., 2009. Stimuli responsive liquid crystals provide on-demand drug delivery in vitro and in vivo. J. Control. Release 135, 218–226. http://dx.doi.org/10.1016/j.jconrel.2009.01.009.

Graham, P.D., Brodbeck, K.J., McHugh, A.J., 1999. Phase inversion dynamics of PLGA solutions related to drug delivery. J. Control. Release 58, 233–245.

Holmberg, K., Shah, D.O. (Dinesh O., Schwuger, M.J. (Milan J. (Eds.), 2002. Handbook of applied surface and colloid chemistry, Applied surface and colloid chemistry. Chichester, England, Chichester, England.

Huang, T.C., Toraya, H., Blanton, T.N., Wu, Y., 1993. X-ray powder diffraction analysis of silver behenate, a possible low-angle diffraction standard. J. Appl. Crystallogr. 26, 180–184. http://dx.doi.org/10.1107/S0021889892009762.

Ilavsky, J., 2012. Nika: software for two-dimensional data reduction. J. Appl. Crystallogr. 45, 324–328. http://dx.doi.org/10.1107/S0021889812004037.

Ki, M.H., Lim, J.L., Ko, J.Y., Park, S.H., Kim, J.E., Cho, H.J., Park, E.S., Kim, D.D., 2014. A new injectable liquid crystal system for one month delivery of leuprolide. J. Control. Release 185, 62–70. http://dx.doi.org/10.1016/j.jconrel.2014.04.034.

Lim, J.L., Ki, M.H., Joo, M.K., An, S.W., Hwang, K.M., Park, E.S., 2015. An injectable liquid crystal system for sustained delivery of entecavir. Int. J. Pharm. 490, 265–272. http://dx.doi.org/10.1016/j.ijpharm.2015.05.049.

Mezzenga, R., Meyer, C., Servais, C., Romoscanu, I., Sagalowicz, L., Hayward, R.C., Romoscanu, A.I., 2005. Shear rheology of lyotropic liquid crystals: a case study shear rheology of lyotropic liquid crystals: a case study. Liq. Cryst. 3322–3333. http://dx.doi.org/10.1021/la046964b.

Patel, R.B., Solorio, L., Wu, H., Krupka, T., Exner, A.A., 2010. Effect of injection site on in situ implant formation and drug release in vivo. J. Control. Release 147, 350–358. http://dx.doi.org/10.1016/j.jconrel.2010.08.020.

Qiu, H., Caffrey, M., 2000. The phase diagram of the monoolein/water system: metastability and equilibrium aspects. Biomaterials 21, 223–234. http://dx.doi.org/10.1016/S0142-9612(99)00126-X.

Rappolt, M., Hickel, A., Bringezu, F., Lohner, K., 2003. Mechanism of the lamellar/inverse hexagonal phase transition examined by high resolution x-ray diffraction. Biophys. J. 84, 3111–3122. http://dx.doi.org/10.1016/S0006-3495(03)70036-8.

Siegel, D.P., Epand, R.M., 1997. The mechanism of lamellar-to-inverted hexagonal phase transitions in phosphatidylethanolamine: implications for membrane fusion mechanisms. Biophys. J. 73, 3089–3111.

Siegel, D.P., 1986. Inverted micellar intermediates and the transitions between lamellar, cubic, and inverted hexagonal lipid phases. I. Mechanism of the L alpha—HII phase transitions. Biophys. J . 49, 1155–1170. http://dx.doi.org/10.1016/S0006-3495(86)83744-4.

Solorio, L., Exner, A.A., 2015. Effect of the subcutaneous environment on phase-Sensitive in situ-Forming implant drug release, degradation, and microstructure. J. Pharm. Sci. 104, 4322–4328. http://dx.doi.org/10.1002/jps.24673.

Solorio, L., Babin, B.M., Patel, R.B., Mach, J., Azar, N., Exner, A.A., 2010. Noninvasive characterization of in situ forming implants using diagnostic ultrasound. J. Control. Release 143, 183–190. http://dx.doi.org/10.1016/j.jconrel.2010.01.001.

Solorio, L., Olear, A.M., Hamilton, J.I., Patel, R.B., Beiswenger, A.C., Wallace, J.E., Zhou, H., Exner, A.A., 2012a. Noninvasive characterization of the effect of varying PLGA molecular weight blends on In Situ forming implant behavior using ultrasound imaging. Theranostics 2, 1064–1077. http://dx.doi.org/10.7150/thno.4181.

Solorio, L., Olear, A.M., Zhou, H., Beiswenger, A.C., Exner, A.A., 2012b. Effect of cargo properties on in situ forming implant behavior determined by noninvasive ultrasound imaging. Drug Deliv. Transl. Res. 2, 45–55. http://dx.doi.org/10.1007/s13346-011-0054-y.

Tiberg, F., Joabsson, F., 2010. Lipid liquid crystals for parenteral sustained-release applications: combining ease of use and manufacturing with consistent drug. OnDrugDelivery (May), 9–12.

Xu, Y., Li, V., Li, J., Abraham, A., Pan Langenbucher, D.G., 2016. Characterization of a liquid crystal system for sustained release of a peptide. 2016 AAPS Annual Meeting and Exposition.